Mechanical behavior of silty soils of the Venice lagoon as a function of their grading characteristics

Simonetta Cola and Paolo Simonini

Abstract: The main feature of the shallowest quaternary basin of the well-renowned historic city of Venice, Italy and its surrounding lagoon, is the presence, apparently without any regular trend in depth and site, of a predominant silt fraction. This is always combined with clay and (or) sand, forming a chaotic and erratic interbedding of different sediments whose mineralogy is however variable in a relatively narrow range due to a unique geological origin and a common depositional environment. After a brief description of the basic soil indexes of the Venice lagoon soil, the present study, based on a comprehensive geotechnical laboratory investigation, describes the range of variation of the most relevant time-independent geotechnical properties. Moreover, a new grain size index, combining the geometrical characteristics of the particle distribution, is introduced. It is shown that the soil response at large and very small strains can be related to this grain size index, which appears to be able to include the influence of the soil grading on the description of the overall mechanical behavior.

Key words: silt, mechanical behavior, Venice soil, grain-size index, laboratory investigation, critical state parameters.

Résumé : La caractéristique principale du bassin quaternaire le moins profond de la célèbre cité de Venise, Italie, et de son lagon environnant est la présence d'une fraction prédominante de silt, sans apparemment aucune tendance régulière de profondeur et de site. Cette fraction est toujours combinée avec de l'argile et (ou) du sable, formant un interlitage de différents sédiments dont la minéralogie est cependant variable dans une plage relativement étroite à cause de son origine géologique unique et de son environnement commun de déposition. Après une brève description des principaux indices des sols du lagon de Venise, la présente étude basée sur une investigation géotechnique élaborée en laboratoire décrit la plage de variations des propriétés géotechniques les plus pertinentes indépendantes du temps. De plus, on introduit un nouvel indice granulométrique combinant les caractéristiques géométriques de la courbe granulométrique. On montre que la réponse du sol à de grandes et très faibles déformations peut être mise en relation avec cet indice granulométrique, ce qui semble pouvoir inclure l'influence de la grosseur des grains sur la description du comportement mécanique global.

Mots clés : silt, comportement mécanique, sol de Venise, indice granulométrique, investigation en laboratoire, paramètres d'état critique.

[Traduit par la Rédaction]

Introduction

The historic city of Venice (Italy) and the surrounding lagoon, whose present configuration is shown in Fig. 1, is suffering overall rapid deterioration. This is caused mainly by an increase in the incidence of flooding due to the eustatic sea level rise, coupled with a natural and man-induced subsidence, the latter having made significant headway between 1946 and 1970 (Rowe 1973; Ricceri and Butterfield 1974).

The importance of preserving the historic city has therefore stimulated the proposal of numerous technical solutions, including movable gates located at the three lagoon inlets to control water levels within the lagoon.

To design the movable gates, studies on the geotechnical characterization of the lagoon soils have been undertaken (Ricceri 1997). A test site was selected from these studies, at the Malamocco inlet (Fig. 1), referred to here as the Malamocco test site (MTS), which could be considered as typical and representative of the entire lagoon area. Several geotechnical investigations, including deep borehole and in situ tests such as piezocone, dilatometer, self-boring pressuremeter, and cross and down hole tests were concentrated and carried out on contiguous verticals at the MTS.

Some of the preliminary results concerned mainly with the laboratory investigations and the applicability of some of the in situ testing methods have already been published

Received 13 March 2001. Accepted 9 January 2002. Published on the NRC Research Press Web site at http://cgj.nrc.ca on 16 July 2002.

S. Cola and P. Simonini.[1] Department of Hydraulic, Maritime, Environmental and Geotechnical Engineering, University of Padova, Via Ognissanti, 39, 35129 Padova, Italy.

[1]Corresponding author (e-mail: paolo.simonini@unipd.it).

 DOI: 10.1139/T02-037

Fig. 1. General view of the Venice lagoon and location of the MTS.

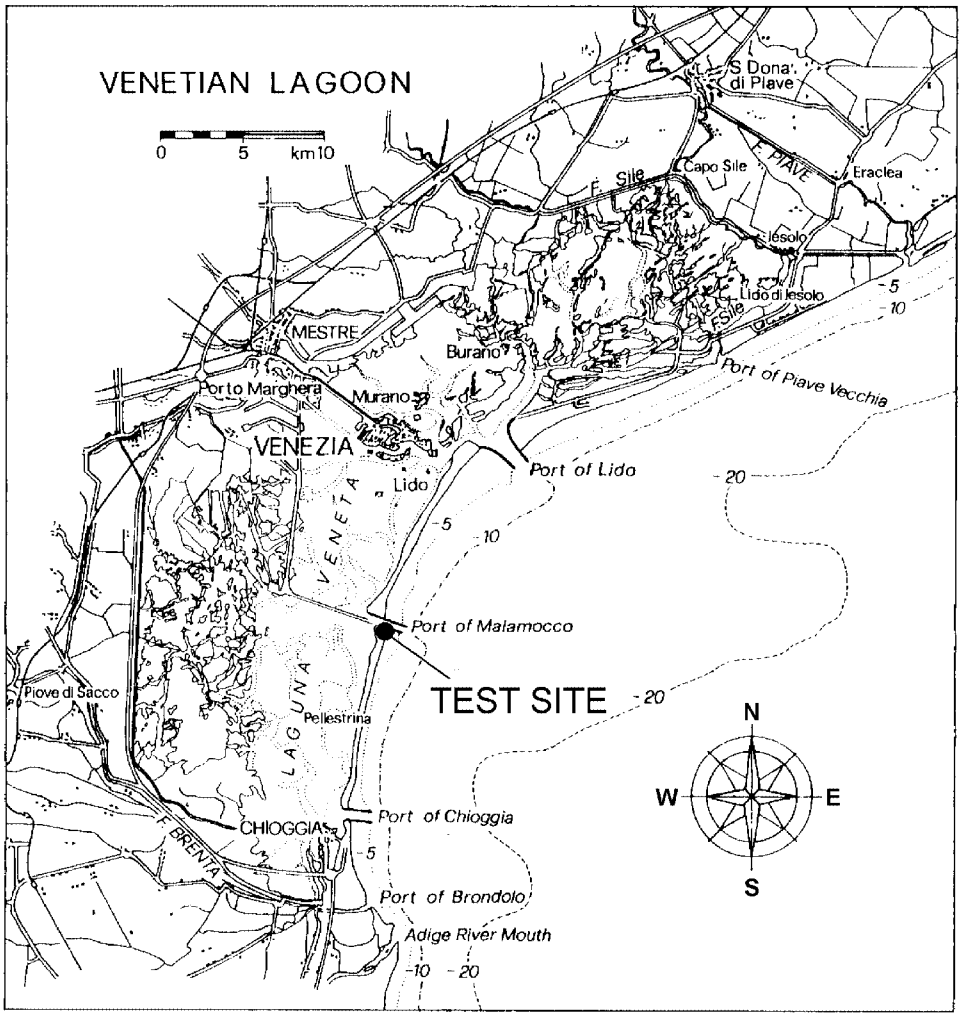

(Cola and Simonini 1999; Simonini and Cola 2000; Ricceri et al. 2002).

From the geotechnical investigations carried out so far, it appears that the main feature of the Venice lagoon soil is the presence of a predominantly silt fraction; this being a consequence of mechanical degradation of the original sand particles.

The silt is always combined with clay and (or) sand, forming a chaotic interbedding of different sediments, whose basic mineralogical characteristics are however, variable from site to site, in a relatively narrow range due to a unique geological origin and common depositional environment.

These silty soils present intermediate characteristics between fine and coarse grained soils. Namely, they are poorly structured materials and highly sensitive to stress-relief due to sampling. Specimens can however be trimmed for mechanical testing in the same way as for cohesive soils. Due to a very complex depositional history, the silty fraction in the Venice soils is combined with clay and (or) sand without any regular pattern with depth, which leads to highly heterogeneous soil conditions.

Firstly, the present study is aimed at evaluating the range of variation of the most relevant time-independent mechanical properties of the Venice lagoon soils through a comprehensive experimental program, consisting of 1D compression tests, drained and undrained triaxial tests, resonant column tests, and bender element measurements carried out in the laboratory on samples coming from the MTS. Secondly, an attempt at describing its behaviour within a common framework is presented and discussed. In particular, the soil parameters at large and very small strains are related to a new grain-size index that is a combination of some basic grain distribution properties.

Brief geological history of the Venice lagoon

The quaternary basin reaches depths of approximately 800 m over the entire lagoon area. During the Quaternary Period, the lagoon area underwent alternating periods of marine transgression and regression, hence both marine and continental sediments coexist. The deposits forming the upper 50–60 m below mean sea level (m.s.l.), the depth of interest to us, are characterized by a complex system of interbedded sands, silts, and silty clays, deposited during the last glacial period of the Pleistocene Epoch (i.e., the Würm Period) when the rivers transported fluvial material from the Alpine ice fields. The Holocene Epoch is only responsible for the shallowest lagoon deposits.

Fig. 2. Soil profile, basic properties, and stress history at the MTS.

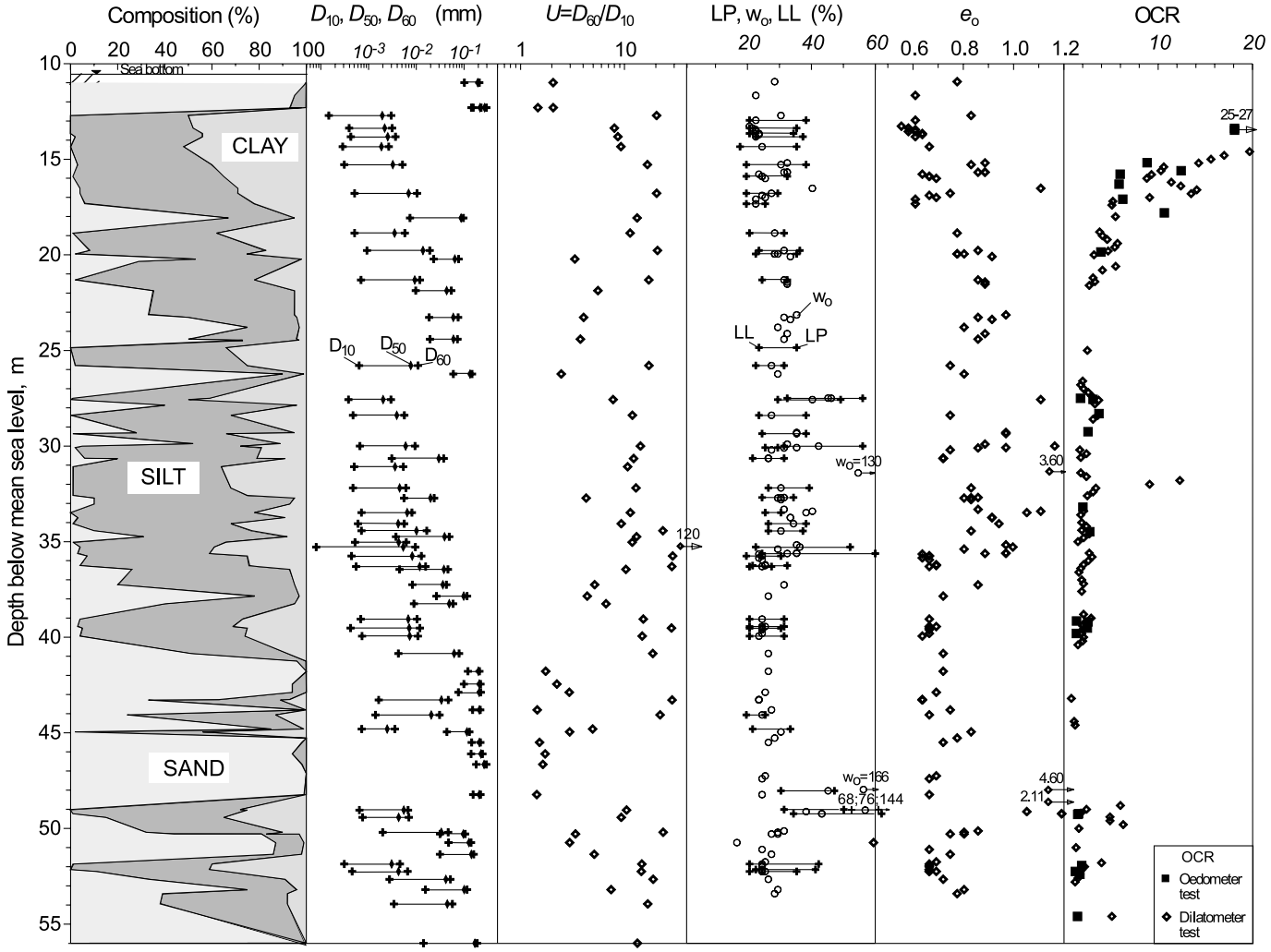

The top layer of Würmian deposits is composed of a crust of highly overconsolidated (OC) lay, commonly referred to as *caranto*, in which many historical Venetian buildings are founded. This layer was subjected to overconsolidation as a result of oxidation during the 10 000-year emergence of the last Pleistocenic glaciation. The OC crust of *caranto*, lying at depths ranging between 5 and 12 m below m.s.l., shows thicknesses varying from a few centimetres to some metres and is slightly sloping towards the shoreline.

Some other deeper OC layers might also be found. Their presence is probably the result of temporaneous oscillations of the sea level during the Wurmian period.

Soil profile, basic properties, and stress history at the MTS

Soil profile and basic indexes

Figure 2 shows the soil composition with depth at the MTS (ground level at the MTS is at 10.5 m below m.s.l.) assessed from grain-size analyses.

The second column reports the diameters D_{60}, D_{50}, and D_{10} of the grain size distributions. Clay fraction content CF can be immediately estimated from the composition depicted in the first column. The third column shows the non-uniformity coefficient $U = D_{60}/D_{10}$.

Atterberg limits, reported in the fourth column together with the natural water content w_o, are characterized by average values of the liquid limit LL and of the plasticity index PI equal to 369% and 147%, respectively.

The cohesive soils generally are characterized by low activity A = PI/CF; more particularly, the great majority of samples falls in the range $0.25 < A < 0.50$, a few of them in the range $0.50 < A < 0.75$, and some organic samples show activity $A > 0.75$.

The in situ void ratio e_o is also reported in Fig. 2. Note that e_o lies in the range approximately between 0.7 and 1.0 from 19 to 36 m below m.s.l.; at greater depths it is somewhat lower and falls in the range 0.6–0.75. Higher values are due to laminations of organic soils included in the cohesive formations.

The specific gravity G_s was determined on several samples and its average value turned out to be equal to 2.77±0.03.

Characteristics of the sediments

For classification purposes, the soil types have been reduced to the following three: medium to fine sand (SP-SM),

Fig. 3. Typical grain-size distributions of the groups SM-SP, ML, and CL.

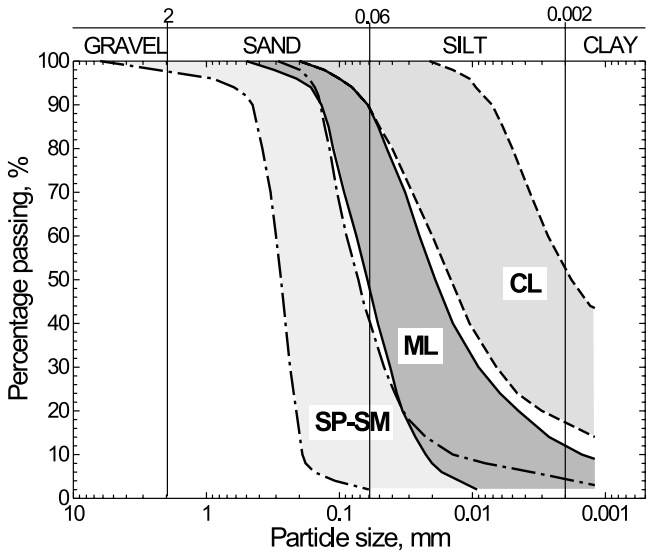

Fig. 4. Typical grain-size distributions and relative mineralogical compositions.

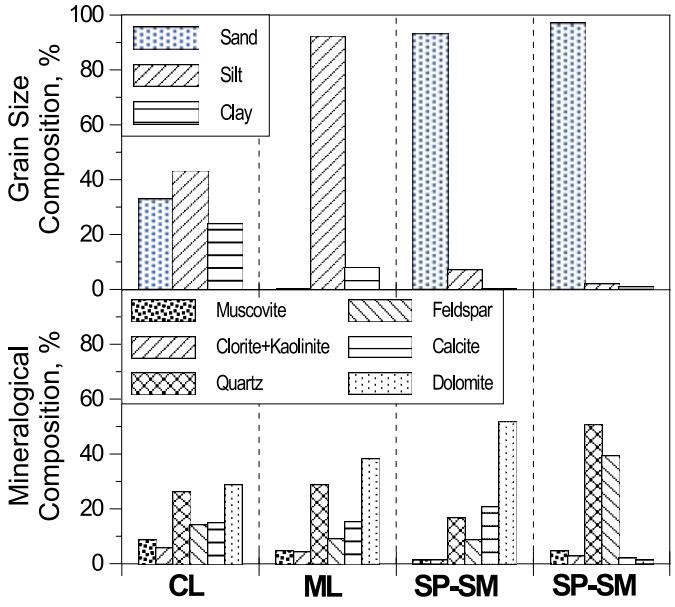

silt (ML), and very silty clay (CL), according to the Unified Soil Classification System. The sands appeared to be relatively uniform, but moving towards finer materials, the grain-size curves display a larger range of particle diameters, as shown in Fig. 3.

The predominance of silty and sandy fractions can be clearly appreciated at the MTS. From borehole log and particle size analyses, the three classes of soils apparently occur in proportions of 35% sand, 20% silts, 40% very silty clays, and 5% medium plasticity clays and peat. Note that from the soil profile in Fig. 2, percentages of silt exceeding 50% are present in 65% of the samples analyzed.

Typical grain size distributions are compared with the relative mineralogical compositions in Fig. 4. It can be noted that SP-SM materials provide two types of mineralogical

Fig. 5. Shape of particles of (*a*) sand and (*b*) silt from an electronic microscope.

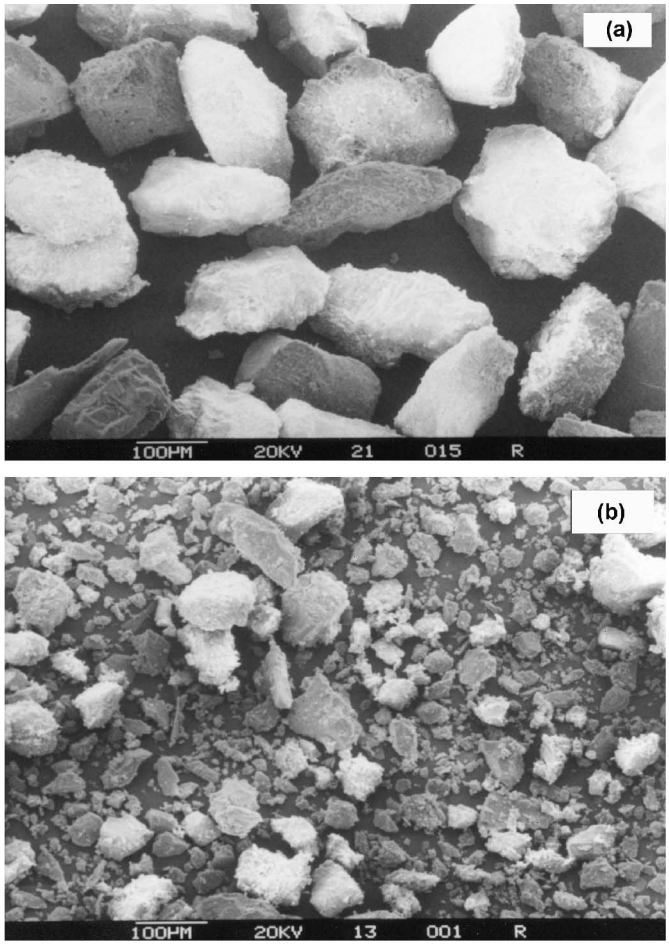

composition, namely the carbonatic and the siliceous. When the carbonate and quartz-feldspar fractions decrease, the clay minerals increase, although they never exceed 30% in any sample. Clay minerals are mainly composed of illite, mainly 2M muscovite, with chlorite, kaolinite, and smectite acting as secondary materials. A mixture of these minerals without any prevailing component characterizes the ML and CL soils.

Using the same degree of enlargement, Figs. 5*a* and 5*b* show typical shapes of sand and silt particles, respectively. The mean rounding index of the grains ranges between 0.23 and 0.34 and seems to remain independent of size; quartz and feldspar grains are generally angular, suggesting they were not transported for any extended length of time.

Stress history

The overconsolidation ratio OCR, plotted in the last column of Fig. 2, was evaluated on the basis of an estimate of preconsolidation stress from oedometric tests using the traditional Casagrande construction. Many difficulties were encountered in applying the method to the majority of the samples (excluding a few plastic samples) because of a low-pronounced yielding curvature. This is probably due to the influence of sampling disturbance together with the silty nature of the sediments, particularly influenced by the stress

relief due to sampling. Other methods were also applied to estimate preconsolidation stress from oedometric curves, such as that suggested by Becker et al. (1987), but satisfactory results were obtained only in the case of the more plastic materials.

The presence of a certain degree of disturbance, mostly related to the nonstructured nature of these soils, was assessed by observing (as proposed by Andersen and Kolstad (1979)) that the vertical strain in oedometric compression at the overburden stress turned out to be somewhat higher than some of the reference values suggested by Holtz et al. (1986).

Therefore, additional OCR values, reported in Fig. 2, were needed to provide a more significant and continuous profile with depth; they were obtained using the flat dilatometer test (Marchetti 1980) performed at the MTS. Some problems could be associated with the use of the dilatometer in estimating OCR for soils with complex stress histories (Smith and Houlsby 1995); Marchetti (1980) suggests however, that the error in assessing OCR is reduced for soils with characteristics similar to those of the Venetian silts.

A general decrease with depth of OCR can be noted with the deeper formations remaining slightly overconsolidated. The higher values close to the ground level are due to the *caranto*. Some deeper layers show higher values of OCR: probably for these soils, as for *caranto*, the overconsolidation was caused by superficial oxidation during the glacial periods. Excluding the highly OC formations above, the main parts of the cohesive soil layers or laminations are slightly overconsolidated with smaller variations of OCR, which lies approximately in the range between 1.2 and 3.7 (average value = 2.3).

Laboratory testing program

An extensive geotechnical laboratory investigation was carried out on the samples obtained from the MTS. It should be emphasized that the very heterogeneous nature of the Venice soils required a relatively large number of tests to define even the simplest properties with a certain degree of accuracy.

The experimental program consisted mainly of 1D compression tests, drained and undrained triaxial compression tests, and resonant column tests with a "fixed-free" apparatus.

Estimations of shear wave velocity have also been performed on some of the triaxial samples using a bender element system with piezoceramic elements embedded in the base pedestal and in the top plate of the triaxial apparatus.

A local measurement system, composed of four axial plus two radial noncontact displacement transducers with targets applied onto the membrane, was used in the triaxial cell to measure axial and radial displacements, respectively, directly on the soil specimens. This system was adopted to accurately measure the full range of deformation from very small strains up to failure.

Specimens were obtained from standard (100 mm) and large diameter (220 mm) Osterberg samples. In the case of sand, specimens were prepared by pushing a tube into the core and then freezing them. After being positioned in the triaxial cell, they were allowed to thaw before undergoing saturation. Silty and clayey specimens were similarly prepared, leaving out the freezing–thawing sequence. The specimens were typically 50–70 mm in diameter with a height–diameter ratio equal to 2. The specimen dimensions for the 1D tests were 50–70 mm in diameter and 20 mm in height.

It should be pointed out that the main difficulty in preparing the experimental program was the selection of relatively homogeneous samples representative of each of the three classes of soil. In fact, even within a 60-cm long core, the soil composition could change significantly, ranging from very silty clay to silts or sandy silts. Therefore, the possibility of testing, as is commonly done, on triple sets of homogeneous specimens was very low, except for a few particular cases involving sands. Nevertheless, the number and types of tests carried out so far seemed to provide us with the basic material parameters for some interesting considerations on overall behaviour, and more particularly on its dependence on some of the basic properties described in the following section.

Basic framework to describe the observed soil behaviour

The observed predominance of the sandy-silty fraction suggested, as a preliminary hypothesis, that the material response under compression and shear may be governed by the mechanical interaction between the particles rather than by electrochemical action.

In addition, the following basic assumptions are used here to evaluate the response of the Venetian soils:

(*a*) The 1D response can be interpreted using the tangent constrained modulus, which is assumed to be a function of the vertical effective stress.

(*b*) At large strains, the material deforms in critical condition, that is, shearing can progress at constant volume without any further changes in stress or void ratio.

(*c*) The critical stress ratio takes the same value of the phase transformation stress ratio, the latter being the ratio at which the soil deforms instantaneously at constant volume.

(*d*) A unique linear relationship between the void ratio and the logarithm of the hydrostatic stress at the critical state is assumed within the stress range used in the tests.

(*e*) The peak strength depends on the position of the current in situ void ratio with respect to the critical condition at the same hydrostatic stress level.

(*f*) A small region exists within which the soil deforms elastically.

(*g*) The selected material parameters can be related to a material index that accounts for the grading characteristics of the soil.

These assumptions will be briefly described in the following sections.

1D compression

Instead of using a stress-independent index such as the slope of the compression line in the $e - \log\sigma'_v$ plane (where σ'_v is the vertical stress), the constrained modulus M, tangent to the e–σ'_v curve, was adopted

$$[1] \qquad M = -\left[(1+e)\frac{d\sigma'_v}{de}\right]$$

As suggested by Janbu (1963), the constrained modulus may be expressed as a function of the current vertical effective stress

$$[2] \qquad \frac{M}{p'_{ref}} = C\left(\frac{\sigma'_v}{p'_{ref}}\right)^m$$

where C and m are two experimental constant and p'_{ref} is a convenient reference mean effective stress taken to be equal to 100 kPa. This equation was preferred because of its simplicity and applicability to a large variety of soils ranging from clays to soft rocks.

Shear response

It is assumed that the critical friction angle, ϕ'_c, can be reliably obtained from standard triaxial compression tests, such as those carried out in this experimental program. The frictional dependence within the range of examined stress is expressed by the linear relationship between the hydrostatic stress p' and the deviatoric stress q

$$[3] \qquad q = \frac{6\sin\phi'_c}{3-\sin\phi'_c}p'$$

which is the expression of the critical state line (CSL) in compression.

Another important value of the mobilized friction angle is the angle ϕ'_{PTP} assessed at the phase transformation stress ratio, also called the phase transformation point (PTP) (Tatsuoka and Ishihara 1974; Ishihara et al. 1975), a particular stress condition in which the material begins to dilate after the end of the initial contractant phase.

According to the stress-dilatancy theory of Rowe (1962) and the steady state concept for undrained behaviour described by Been and Jefferies (1985) and Been et al. (1991), the PTP ratio should be the same as the critical stress ratio. However, the PTP ratio was simpler to estimate in our tests because it was reached at an early stage of the test, whereas the critical state required large deformations.

Due to the direct link with relative density and other related parameters, we also preferred, for our own soils, to formulate the CSL in terms of void ratio rather than specific volume (Jefferies 1993; Jefferies and Been 2000)

$$[4] \qquad e_c = e_{ref} - \lambda_c \log\frac{p'}{p'_{ref}}$$

where λ_c is the slope of the CSL in the $e - \log p'$ plane and is 2.3 times the slope of the CSL in the classical formulation of the critical state theory.

The material parameter e_{ref} is the void ratio at the reference mean effective stress of p'_{ref} = 100 kPa. This value, instead of holding the classical value of specific volume at 1 kPa, which was selected because of its simpler determination, is less affected by experimental errors in relation to the range of stress considered in this experimental program.

On the CSL, the rate of dilation is zero and it is reasonable to hypothesize that the dilation rate of all of the soil mixtures is controlled by the volumetric distance between the current state of the soil and the CSL. This concept, originally suggested by Wroth and Bassett (1965) and reproposed by Been and Jefferies (1985), is expressed here by the distance between the current void ratio and the CSL at constant mean effective stress, called the state parameter ψ, where

$$[5] \qquad \psi = e - e_{ref} + \lambda_c \log\frac{p'}{p'_{ref}}$$

For sands, the dilation rate is accepted to be a unique function of the current void ratio. As reported by Houlsby (1991), a simple linear relationship between the maximum dilation rate $(d\varepsilon_v/d\varepsilon_a)_{max}$ and ψ could be rearranged for our purposes in the following form:

$$[6] \qquad \left(-\frac{d\varepsilon_v}{d\varepsilon_a}\right)_{max} = \alpha\psi$$

where $(-d\varepsilon_v/d\varepsilon_a)_{max}$ is the maximum dilation rate at peak strength in triaxial compression (ε_v and ε_a are the volumetric and axial strain, respectively) and α is a positive proportionality constant.

Combining eq. [5] with [6] we have:

$$[7] \qquad \left(-\frac{d\varepsilon_v}{d\varepsilon_a}\right)_{max} = \alpha\left(e - e_{ref} - \lambda_c \log\frac{p'}{p'_{ref}}\right)$$

Equation [7] implies that $(-d\varepsilon_v/d\varepsilon_a)_{max}$ increases as the current void ratio decreases, and decreases as p' increases. This equation can be compared to the empirical expression suggested by Bolton (1986, 1987) for deriving the maximum dilation rate and the peak angle of friction ϕ'_p in triaxial compression

$$[8] \qquad \left(-\frac{d\varepsilon_v}{d\varepsilon_a}\right)_{max} = 0.3I_R$$

and

$$[9] \qquad \phi'_p - \phi'_c = 3I_R$$

with

$$[10] \qquad I_R = I_D[(Q - \ln p'_f) - 1]$$

where $I_D = (e_{max} - e)/(e_{max} - e_{min})$ is the relative density, p'_f is the mean effective stress at failure, and Q is an experimental constant equal to 10 for quartz and feldspar sands and 8 for limestone.

Equations [7]–[10] were used to analyze the experimental data. In analogy with the findings of Bolton (1986) for a great variety of sands, in this study it is assumed that the peak strength is linked with the current value of ψ, and therefore with $(-d\varepsilon_v/d\varepsilon_a)_{max}$), by a simple linear expression, similar to that proposed by Wood et al. (1994)

$$[11] \qquad \phi'_p = \phi'_c - \beta\psi$$

where β is a constant material parameter.

Very small strain behaviour

It is assumed that the soil behaves elastically at very small strain and, therefore, the response can be interpreted in terms of shear stiffness G_{max}, the latter being influenced by the mean effective stress, the OCR, and the void ratio

(Hardin and Black 1969). For sands, low-plasticity, and slightly OC cohesive soils, the effect of the OCR can be considered negligible (Hardin and Drnevich 1972). Therefore, G_{max} can be related to e and p' by the expression

$$[12] \quad \frac{G_{max}}{p'_{ref}} = D f(e) \left(\frac{p'}{p'_{ref}} \right)^n$$

where D is a material constant, $f(e)$ is a void ratio function, n is an exponent and p'_{ref} is the reference stress (100 kPa).

Some relationships have been proposed in the past to express the function $f(e)$ in eq. [12] (e.g., Hardin and Drnevich 1972; Jamiolkowski et al. 1994; Biarez and Hicher 1994; Shibuya and Tanaka 1996). The original expression proposed by Hardin and Drnevich (1972)

$$[13] \quad f(e) = \frac{(2.97 - e)^2}{(1 + e)}$$

was used in this research to analyze the experimental results.

The grain-size index

Attempts to relate the soil mechanical properties to the grading characteristics of incoherent soils have been recently proposed (Miura et al. 1997) for example, by separately considering the influence of variation of D_{50} or U on the overall mechanical behaviour of one or more soils.

Since all of the Venetian sediments originated from one common basic material, namely siliceous–calcareous sand, by crushing and sedimentation (at least up to the very silty clay fraction) it is attempted here to establish an improved relationship between the mechanical properties and the grading characteristics.

The main feature of the grading characteristics of Venetian soils is that the sands are relatively uniform, but moving towards finer materials, the soils become more graded and the grain-size curve displays a larger range. This feature can be better appreciated by observing the variation of U as a function of D_{50}: the coarser the materials, the lower U, whose range increases with decreasing D_{50}. The type of evolution of the grading curve of coarse materials subjected to mechanical actions seems to be confirmed by the recent studies based on a fractal approach by Mc Dowell (1996) and Mc Dowell and Bolton (1998), who have shown the occurrence of this opposite variation of D_{50} and U in crushed sands, expressible in some mathematical form.

On the basis of the above observations, we sought to compare all of the available D_{50} and U data from the MTS investigation, in terms of profiles of D_{50} and U against depth. This is shown in Fig. 6 for all of the (D_{50}, U) couples, displayed using dashed and continuous lines, respectively.

Note that, even if both quantities show oscillations of approximately two orders of magnitude, the profiles of D_{50} and of U are generally characterized by opposite trends with depth, namely, when D_{50} decreases, U increases and vice-versa. This particular correspondence is observed at all depths with some local exceptions.

To take into account the coupled and opposite variation of D_{50} and U into a single parameter, it is convenient to introduce a new grain-size index I_{GS} defined as

Fig. 6. Profiles of mean particle diameter, non-unformity coefficient, and grain-size index at the MTS.

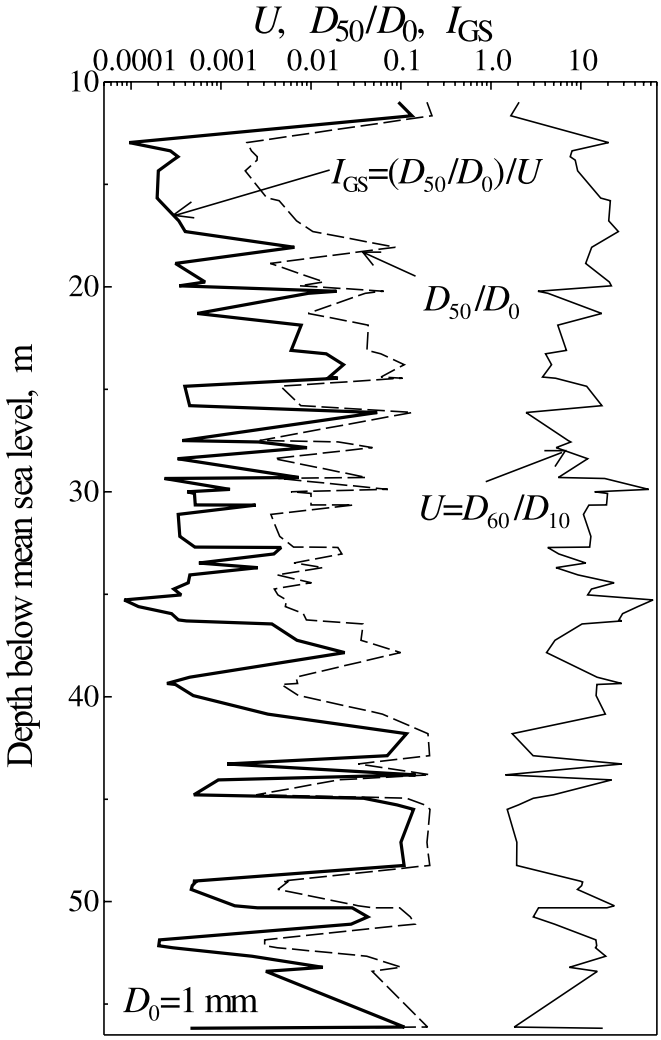

$$[14] \quad I_{GS} = \frac{D_{50} / D_0}{U}$$

where D_0 is a reference diameter, taken as equal to 1 mm.

The advantage of using I_{GS} as a material index instead of D_{50} or U is due to the fact that I_{GS} associates in a unique expression two soil characteristics that influence the response of a given soil in opposite ways. That is, soil strength and stiffness increase with increasing D_{50} and decreasing U.

Note that the significance of I_{GS} is limited only to soil where the CF generally does not exceed 25%. For CF > 25%, electrochemical effects may assume a relevant role in the interaction between soil particles and, therefore, grain size distribution must be associated with another index such as clay fraction, Atterberg limits, or mineral activity.

Analysis and discussion of the experimental results

1D compression

Some of the results of the 1D compression tests carried out on undisturbed samples of sands–silts and very silty

Fig. 7. 1D compression curves for (*a*) SM-SP-ML and (*b*) CL.

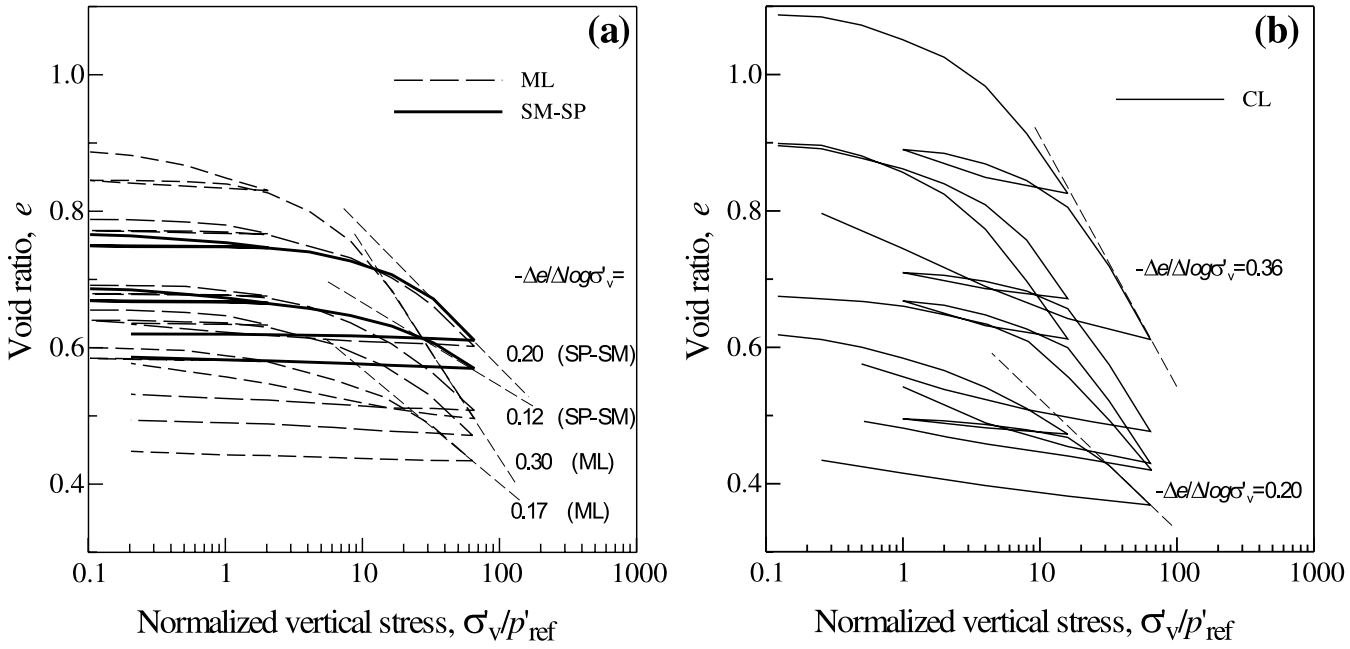

clays are shown in Figs. 7*a* and 7*b*, respectively, in the normalized $e - \log(\sigma'_v/p'_{ref})$ plane. Note the typical response of silty material in compression, characterized by the absence of any clear yield point, which separates the recompression response from that of the virgin compression.

It is interesting to observe that, within the stress range used in these tests and not exceeding 6 MPa, the slope of curves in the virgin compression zone shows a large variation even in the same class of material. For sands it ranges between 0.12 and 0.20; for silts between 0.17 and 0.30, but if we exclude this latter value, the range reduces to between 0.17 and 0.22; for CL the slope is somewhat higher, from 0.20 to 0.36.

To evaluate the dependence of 1D compressibility on the grain size composition and on the stress level, we preferred to consider the constrained modulus M, defined by eq. [1], as a function of vertical stress, as was assumed in eq. [2].

Figure 8 shows the trend of M as a function of σ'_v/p'_{ref} for the three classes of soil. The lowest values correspond to the very silty clays, whereas the highest correspond to the sands, with the intermediates corresponding to the silts.

Note that there are some exceptions to this general trend: soils, classified as CL, show a response typical of ML and vice-versa. These soils lie on the borderline between the two, and therefore, some experimental uncertainties in establishing grain size distribution may lead to an erroneous classification of the sample.

The range of variation of M within each group tends to reduce as the stress level reaches the virgin compression response, except for sands, where the applied stress was not so high as to unify the compression curve in a unique limiting compression line as suggested by Pestana and Whittle (1996).

The experimental constants C and m were estimated for several samples and are reported in Figs. 9*a* and 9*b*, respectively, versus the grain size index I_{GS}. A significant increase

Fig. 8. Constrained modulus versus vertical effective stress.

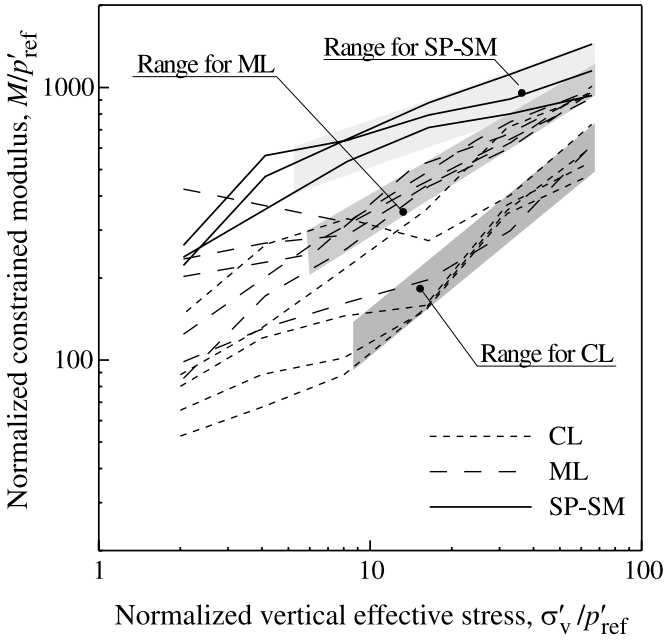

of C with I_{GS} is observed, with a range of 30 around the average regression value. On the contrary, the exponent m decreases slightly with I_{GS}, varying from 0.6 ± 0.1 to 0.4 ± 0.1. The point in Fig. 9*b*, lying well above the range of m was excluded from the analysis of the data because it was from a sample with an activity $A = 0.83$, which is much higher than typical activity values for lagoon sediments.

The trends shown for C and m fit the following equations:

[15*a*] $C = 270 + 56\log I_{GS}$

[15*b*] $m = 0.30 - 0.069\log I_{GS}$

Fig. 9. Constants (*a*) *C* and (*b*) *m* as a function of grain-size index.

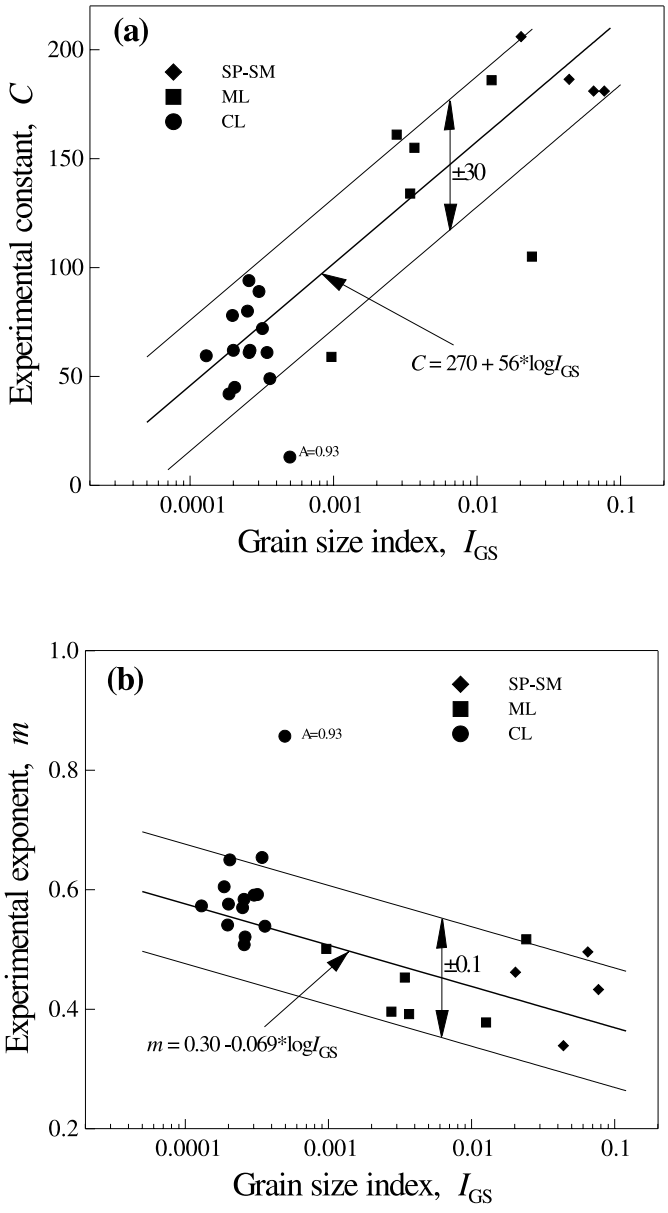

Critical state

Typical results for the majority of the samples tested in undrained triaxial compression are shown in Figs. 10*a* and 10*b* for the extreme classes SM-SP and CL in terms of deviatoric stress q versus axial strain and pore pressure u versus axial strain. The evolution of pore pressure indicates the presence of both contractant and dilatant tendencies during shear, at small and large strains, respectively.

Consequently, with pore pressure trend, the stress paths of the above tests, plotted in the p'–q plane in Fig. 10*c*, move to the left at an early stage of the test and then turn to the right. The PTP indicates the end of the contractant phase, after which the sample exhibited dilatant behavior. The position of the PTP in the p'–q plane was determined by evaluating, at an early stage of compression, the combination of p'–q at which the soil deformed instantaneously at constant pore pressure.

Figure 11*a* shows typical stress–strain curves measured on two triple sets of both SM-SP and CL materials sheared in drained tests. The volumetric strain versus axial strain curves (Fig. 11*b*) showed similar response with an initial contractant behaviour followed by dilation. The stress ratio at which the soil deforms instantaneously with zero volumetric strain rate is considered to have the same meaning as the phase transformation stress ratio assessed in the undrained tests.

Non-dilatant responses were observed in only a few tests performed on samples with higher clay content, but such behavior was not representative of the typical Venetian soil.

All of the values of the PTP ratios, transformed into the mobilized friction angle ϕ'_{PTP}, are plotted against the critical state angle ϕ'_c in Fig. 12 distinguishing between the three classes of soil and between the drained (D) and undrained (U) tests. The data in Fig. 12 do not include all of the performed tests; in some cases the evaluation of the stress ratio at the critical state proved extremely cumbersome due to the absence of continuous deformation at constant stress and void ratio.

As expected, higher values are due to sands and range approximately between 34 and 39°, whereas silty clays show lower values, from 30 to 34°. The critical friction angle of silts covers a larger range, reaching also the upper values of sands. It is interesting to note that, without distinguishing between the three classes of soil or the type of test, a good correspondence exists between ϕ'_{PTP} and ϕ'_c, with scatter from the average value not exceeding 2°.

Pairs (e_c, p') estimated at the critical condition from both drained and undrained tests are displayed in Fig. 13 in a semi-log plot. Sands and silts reach the critical state with a void ratio generally greater than that for silty clay and with no particular difference between them. A particular case is represented by two specimens classified as sand but with a significant fraction of silt (the value of U is labeled on the diagram); their void ratio at critical state is at the lower boundary of the values measured.

Two regression lines, one for both sand and silt and the other for silt clays, are reported in Fig. 13. The couple of parameters (e_{ref}, λ_c) turned out to be equal to 0.918 and 0.066 for SM-SP-ML and to 0.818 and 0.107 for CL, respectively.

The decision to plot all of the data without specifically noting specimens trimmed from the same sample was due to the difficulty (except in a few cases) of establishing well-defined trends in the semi-log plot. The difficulty of finding others among specimens obtained from the same core may probably be due not only to the already discussed heterogeneity of the material but also to the lack of straining uniformity of the sample. In fact, it was only possible to estimate the average void ratio of the sample and not the effective void ratio on the planes of failure, in the cases when they occurred.

However, where the definition of the single CSLs for each set of specimens was reasonably possible, linear regressions were used to estimate the corresponding values of the slope of the CSL and of e_{ref}.

The critical state parameters ϕ'_c, λ_c, and e_{ref} were related to the grain size index I_{GS} with the results sketched in Figs. 14*a*, 14*b*, and 14*c*, respectively. All three parameters are clearly dependent on I_{GS}; this dependence was tentatively expressed

Fig. 10. Typical results in undrained triaxial compression tests for SM-SP and CL materials: (*a*) deviatoric stress versus axial strain, (*b*) pore pressure versus axial strain, and (*c*) deviatoric versus mean effective stress.

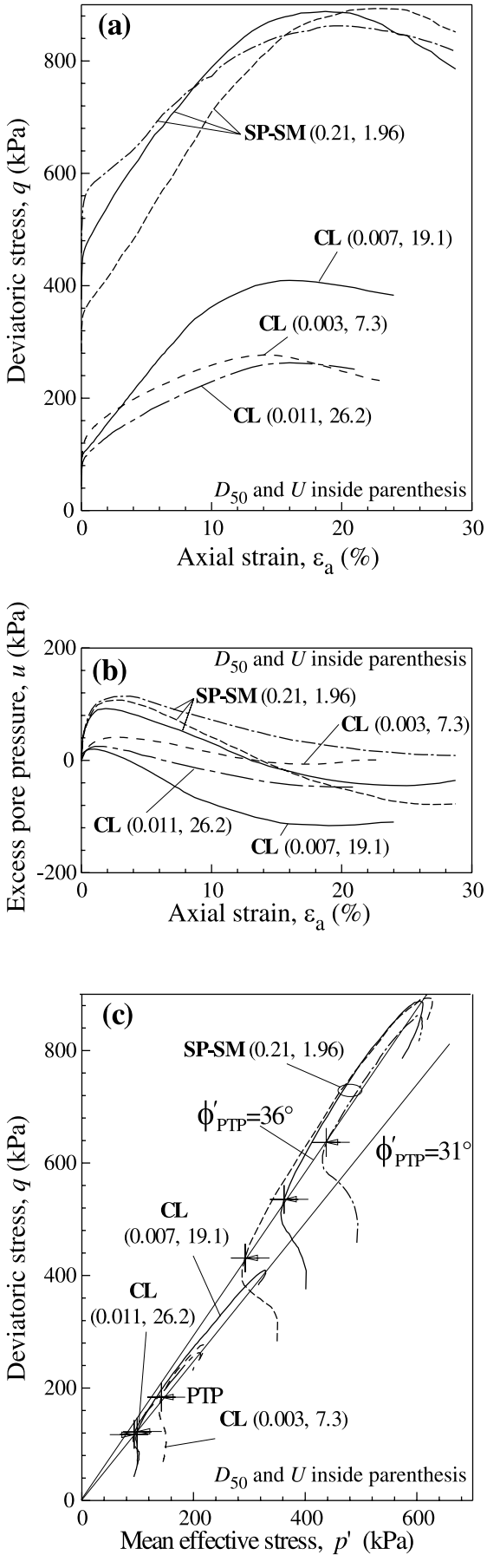

Fig. 11. Typical results in drained compression tests for SM-SP and CL materials: (*a*) deviatoric stress versus axial strain, and (*b*) volumetric strain versus axial strain.

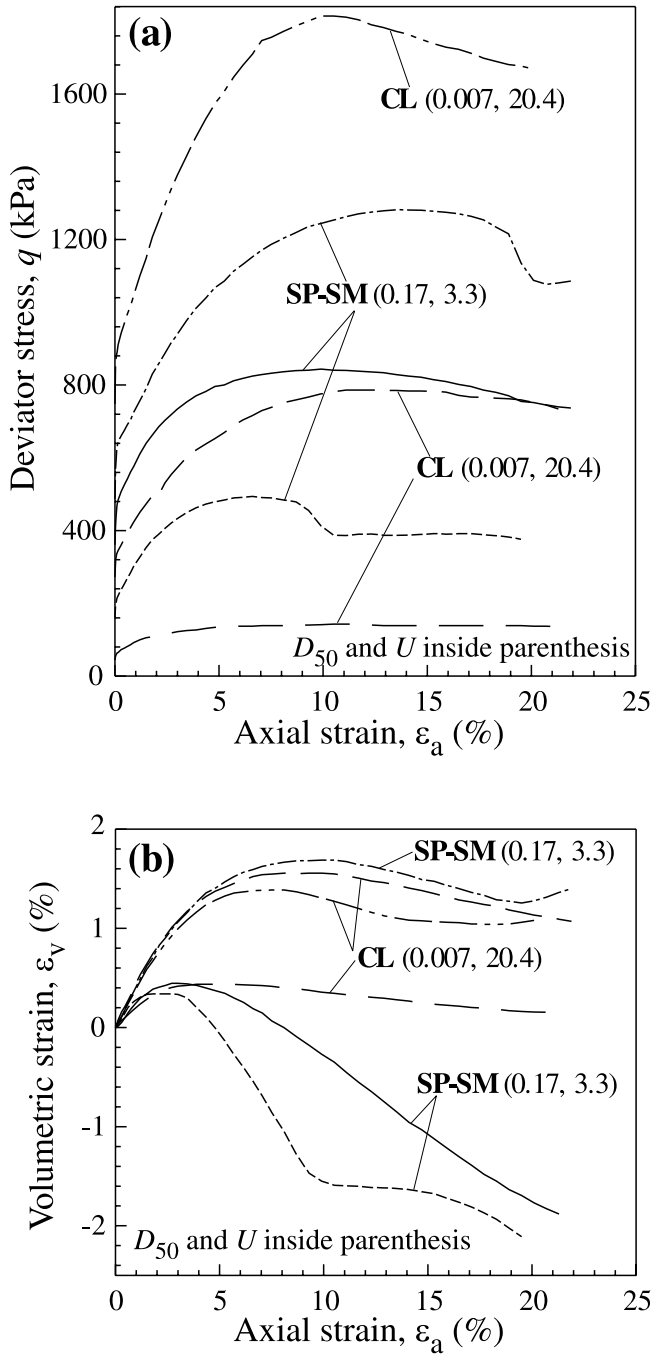

Fig. 12. Critical state angle versus point transformation phase angle for the various classes of soil.

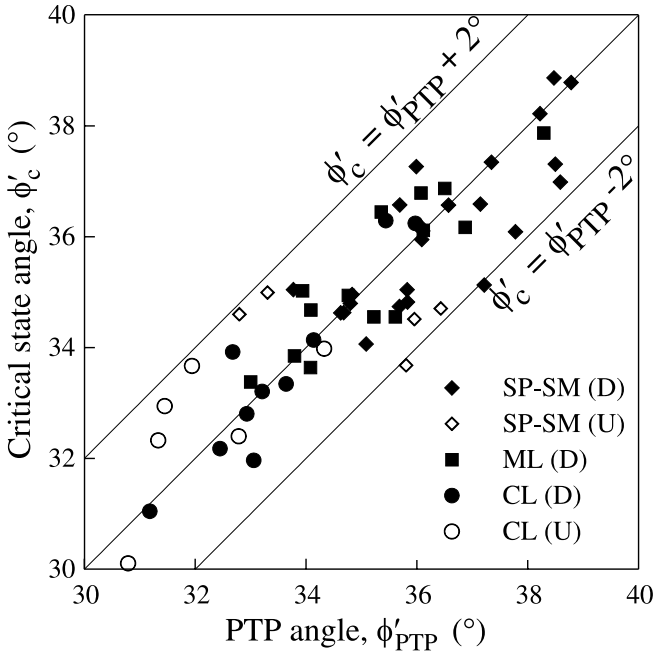

Fig. 13. Critical state line in the log (mean effective stress) – void ratio plane.

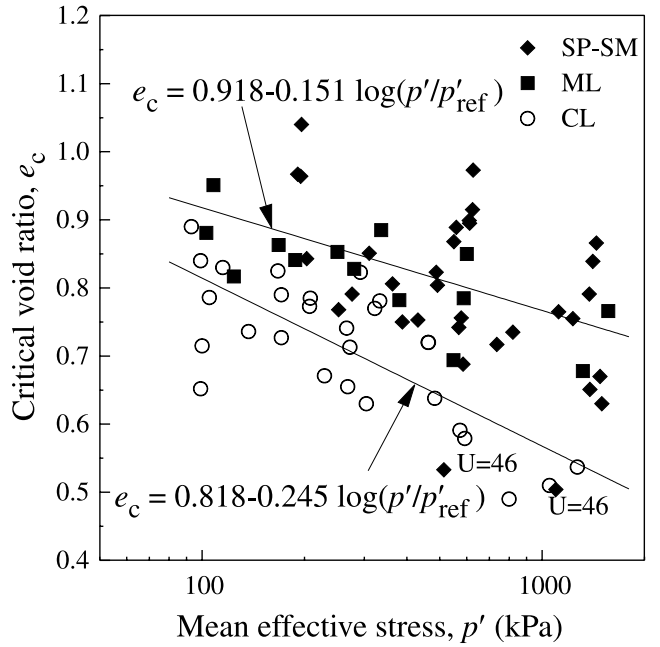

by logarithmic curves drawn on the relative diagrams. The trends, evaluated in the range between $8 \times 10^{-5} \le I_{GS} \le 0.12$, are characterized by the following expressions:

$$[16a] \quad \phi'_c = 38.0 + 1.55 \log I_{GS}$$

$$[16b] \quad \lambda_c = 0.066 - 0.016 \log I_{GS}$$

$$[16c] \quad e_{ref} = 1.13 + 0.10 \log I_{GS}$$

It is interesting to point out that before using the above correlations between the critical state parameters and I_{GS}, attempts have been made to relate the same parameters singularly to D_{50} and U. The results indicated that ϕ'_c, λ_c, and e_{ref} are a function of both quantities but with opposite effects, i.e., ϕ'_c increases with D_{50} and decreases with U.

Dilatancy, peak strength, and state parameter

Figure 15 shows the maximum dilation rate $(-d\varepsilon_v/d\varepsilon_a)_{max}$ measured in triaxial compression tests against the mean effective stress at failure p'_f. The same figure also displays the data of a few samples showing the contractant response; in this case dilatancy values were set to zero and the points were drawn on the p'_f axis.

Features to note are as follows: (*i*) A general decrease of $(-d\varepsilon_v/d\varepsilon_a)_{max}$ with p'_f is observed for both sandy and silty soils. The shaded area includes the majority of data from tests on sands and silts and the few data outside this area are due to silts with high clay fractions (CF is labeled above the dots); (*ii*) No particular distinction is evident between the sand and silt behaviour; (*iii*) Dilatancy vanishes at stress levels beyond about 1 MPa in all samples; and (*iv*) The very silty clays are characterized by very low dilatancy with no particular trend related to p'_f.

Using Bolton's expressions in eqs. [8]–[10], the limits of the shaded area may be marked using the values of $I_R = 0.7[(9 - \ln p'_f) - 1]$ and $I_R = 0.5[(9 - \ln p'_f) - 1]$. This implies that the measured dilatancy should correspond to a relative density I_D in the range 0.5–0.7 with the parameter Q equal to 9.

The difference between peak and critical friction angles $(\phi'_p - \phi'_c)$ is also reported against p'_f in Fig. 16. As observed for dilatancy, the difference between the two angles for sands and silts is highly dependent on the mean stress level. The area including the range of data for these soils is shaded and limited by $\phi'_p - \phi'_c = 3.9 I_R$ with I_D equal to 0.5 and 0.7. The value of 3.9 for the ratio $(\phi'_p - \phi'_c)/I_R$ is somewhat higher than the value of 3 found by Bolton (1986) for a large number of sands. This result may be explained by considering that the Venetian sand and silt are composed of angular grains, thus providing a higher degree of interlocking; whereas the data reported by Bolton (1986) referred to sands characterized by low degrees of angularity (e.g., subangular–subrounded particles of Sacramento river sand; well-rounded grains of Ottawa sand, see Lee and Seed (1967)).

The state parameter ψ defined in eq. [7] was calculated from the experimental data and plotted against $(-d\varepsilon_v/d\varepsilon_a)_{max}$ in Fig. 17. As in Fig. 15, slightly positive values of ψ corresponding to small contractant response were also drawn but in Fig. 17, $(-d\varepsilon_v/d\varepsilon_a)_{max}$ was set equal to zero in these cases.

A decrease in dilatancy with state parameter can be observed. Moreover, a relatively large scatter of data is noted. This is due to the difficulty in making an accurate evaluation of ψ as a result of the uncertainties in estimating the void ratio at the beginning of the shearing stage. Despite the large scatter of data, it is interesting to note that the link between state parameter and dilatancy for SM-SP and ML may be assumed linear in the diagram. Two straight and parallel lines include all of the data for the two classes in Fig. 17. The slope of these lines represents the parameter α in eq. [7], to which the value of 3.5 can be roughly attributed. This value

Fig. 14. Critical state parameters as a function of grain size index: (*a*) critical state angle, (*b*) slope of the CSL, and (*c*) reference void ratio.

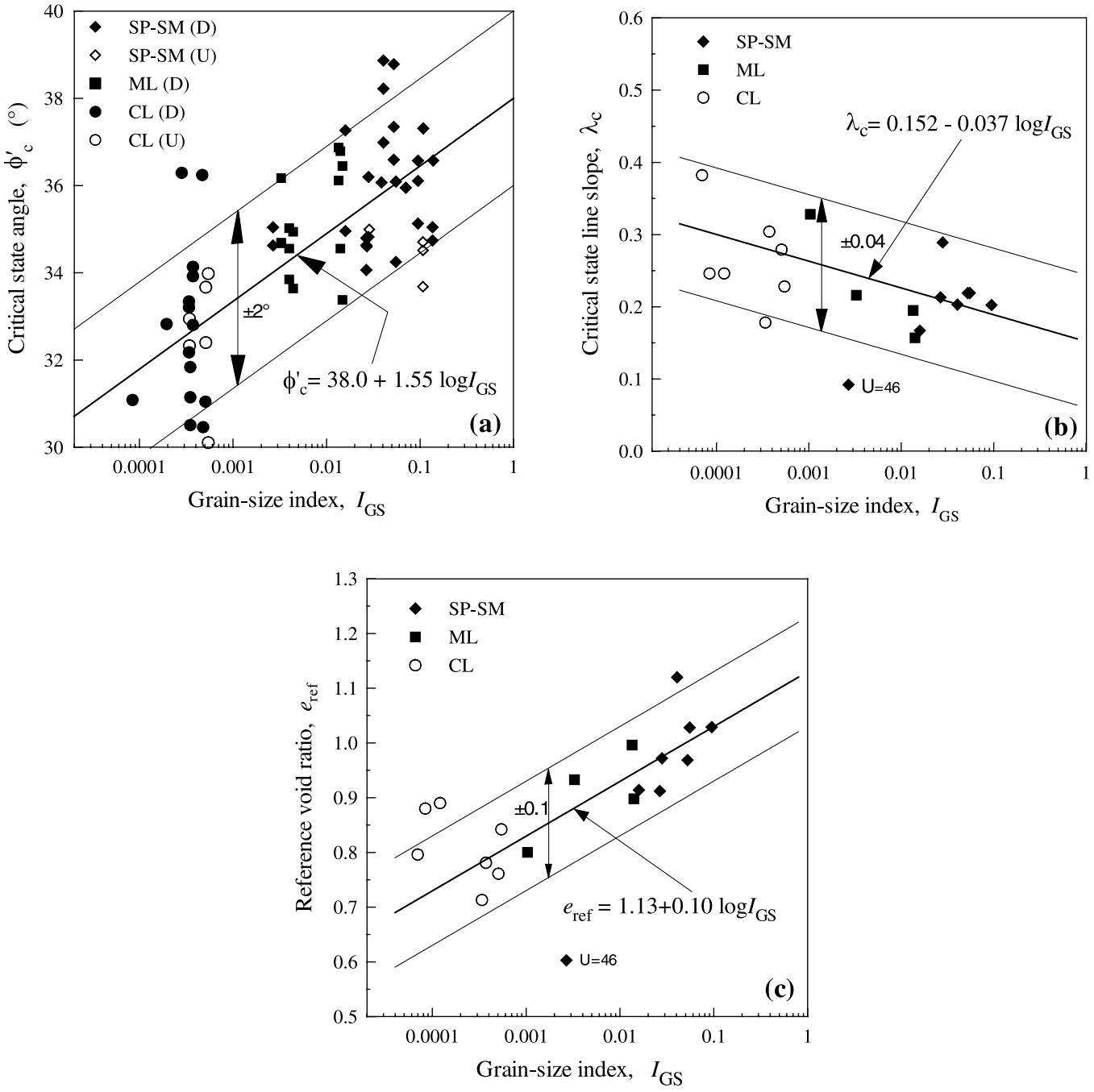

seems to be consistent with the relationship between the state parameter and the dilation rate in the triaxial compression found by Been and Jefferies (1985) for sands with fines content less that 10%.

The dilatancy is generally smaller for very silty clay compared to sands and silts; this may support the dependence of α on the material composition. To evaluate this dependence, slope α was plotted against I_{GS} in Fig. 18. As for the other examined parameters, no substantial differences exist between the values of α for sands and silts. The value of α decreases only when the presence of a clay fraction becomes significant, but unfortunately the data is insufficient for establishing any reliable relationship between the two quantities.

The dependence of ϕ'_p on ψ is considered in Fig. 19. The data are enveloped by two straight lines given by eq. [12] with a slope β of 40 for sands and silts. A similar trend could also be assumed for very silty clay, but in this case, the slope would be characterized by a lower value of β.

Very small strain behavior

In Fig. 20, the experimental values of maximum stiffness G_{max}/p'_{ref}, corrected by $f(e)$ function, are related to the mean effective dimensionless stress p'/p'_{ref}. The data are grouped by soil class and labeled according to the way they were obtained, either from tests using the Bender Element system (BE) or Resonant Column (RC). For each group of soils the

Fig. 15. Maximum dilatancy versus mean effective stress at failure in triaxial compression.

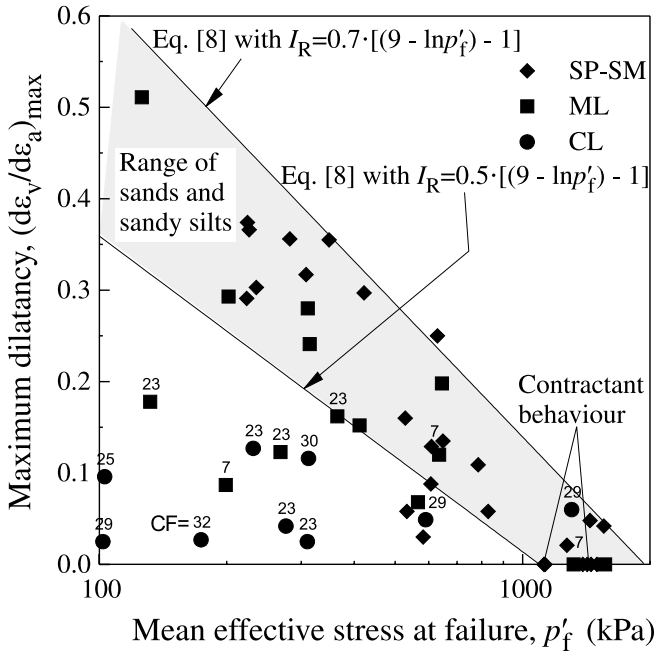

Fig. 16. The difference between critical and peak angle as a function of mean effective stress at failure in triaxial compression.

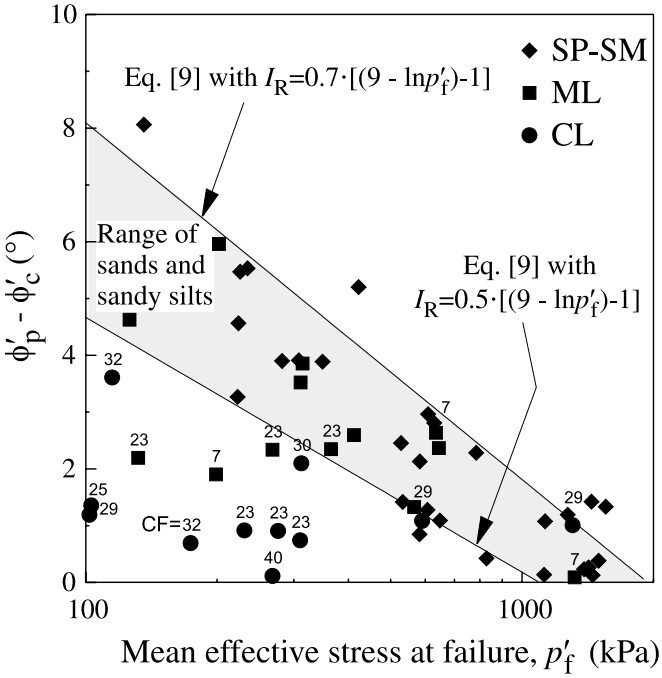

maximum stiffness determined in RC turned out to be lower than that measured with BE. This could probably be due to the greater dynamic strain level imposed in the RC test, as shown by Tatsuoka and Shibuya (1992).

The dependence on p' is indicated in Fig. 20 for each group of data. The exponent n in eq. [12] varies from 0.56 to 0.68, and a value of 0.60 can be reasonably assumed as being representative of the trend for all of the data.

Fig. 17. State parameter versus maximum dilatancy in drained triaxial compression.

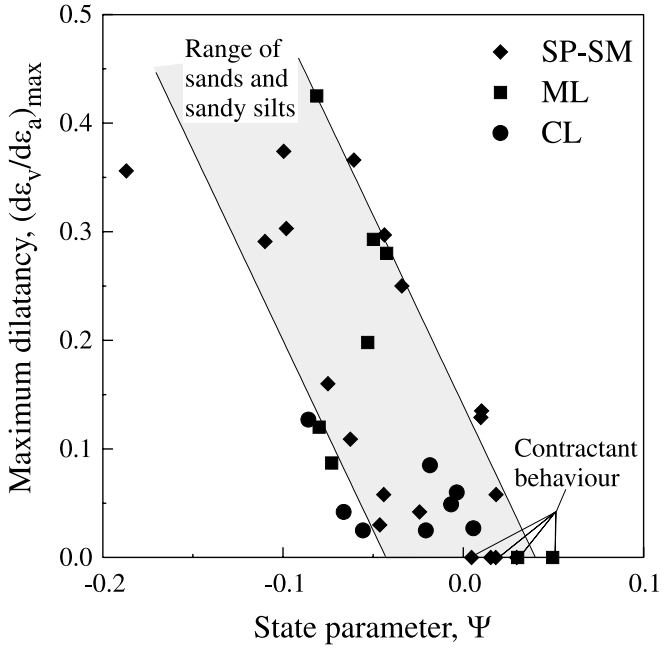

Fig. 18. Slope α versus material composition.

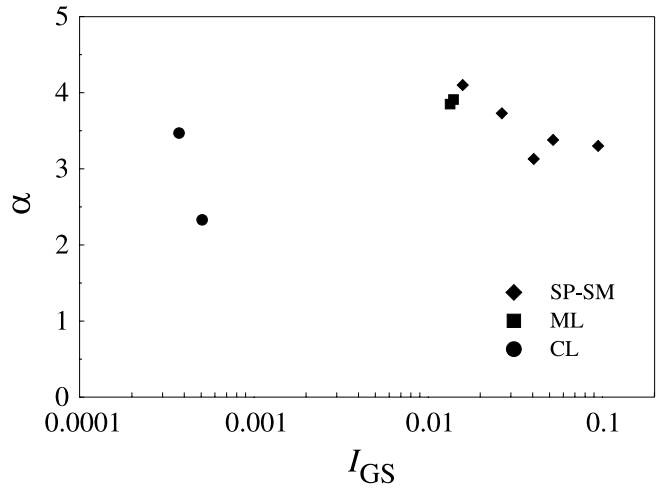

To examine the dependence of the material constant D from eq. [12] on the grain size index, the maximum stiffness was divided by $f(e)(p'/p'_{ref})$ and plotted versus I_{GS} in the semi-log diagram in Fig. 21. All of the data fit on the logarithmic curve with equation

[17] $D = 190 + 10.4 \log I_{GS}$

Note that the grain size index I_{GS} is once more capable of expressing the dependence of maximum stiffness on the three classes of soils.

Concluding remarks

This paper presented an attempt to describe, within a unified approach, the mechanical behavior of Venice lagoon soils, which are mostly composed of heterogeneous mixtures

Fig. 19. Peak angle in triaxial compression as a function of the state parameter.

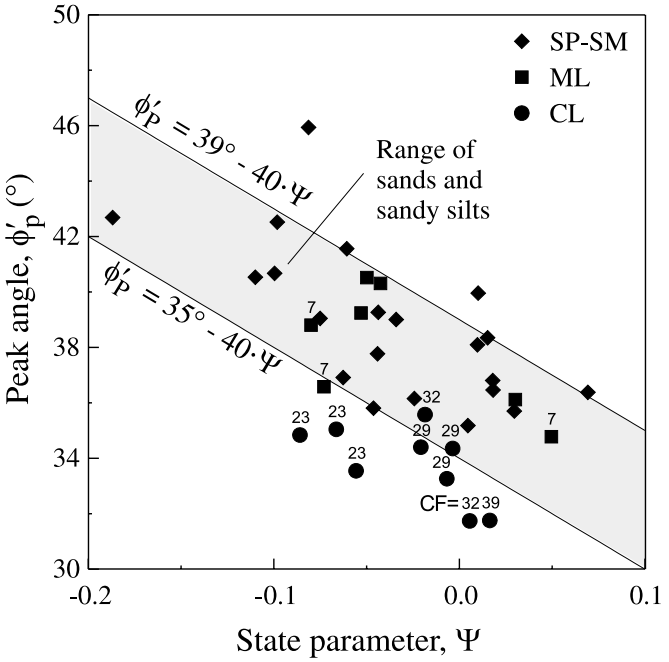

of slightly overconsolidated silt combined with clay and (or) sand.

To evaluate the range in variation of the most relevant time-independent mechanical properties, a comprehensive experimental program was carried out. It should be emphasized that the main difficulty in preparing the experimental program was the selection of relatively homogeneous samples representative of the three classes of Venice soils, namely, medium fine sand (SM-SP), silt (ML), and very silty clay (CL).

From the observations of the nature and origin of the soil sediments and from the analysis of the experimental results, it appears that the overall response of the Venice lagoon soils tested in various conditions could be described in terms of mechanical rather than electrochemical interaction between soil particles, with the exception of a few cases due to plastic clays.

All of the Venetian sediments originated from one common basic material, namely, siliceous-calcareous sand, by crushing and sedimentation, at least as far as the very silty clay fraction. Hence, we attempted to relate the mechanical soil properties to their grading characteristics. The main feature of the latter is that the highly interbedded stratifications are characterized by the presence of sediments, displaying grain-size curves that, moving towards finer materials, show an increase in the nonuniformity coefficient coupled with a reduction of the mean particle diameter.

To draw this opposite variation into one single parameter, a new material parameter was introduced and called the grain-size index I_{GS}. It unites two important grading characteristics of the soils into one single expression.

The relevant mechanical parameters of the Venetian soils were related to their grain-size composition through I_{GS} and the following main observations were made:

Fig. 20. Small strain stiffness versus confining stress for the three classes of soils.

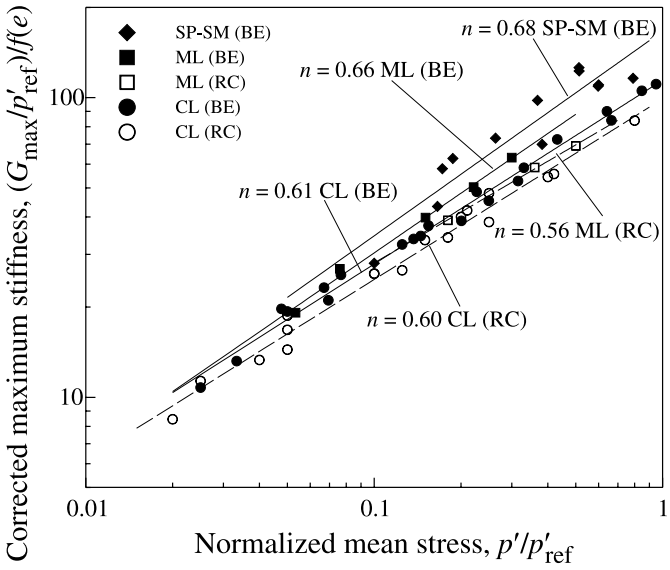

Fig. 21. Dependence of maximum stiffness on the grain size index.

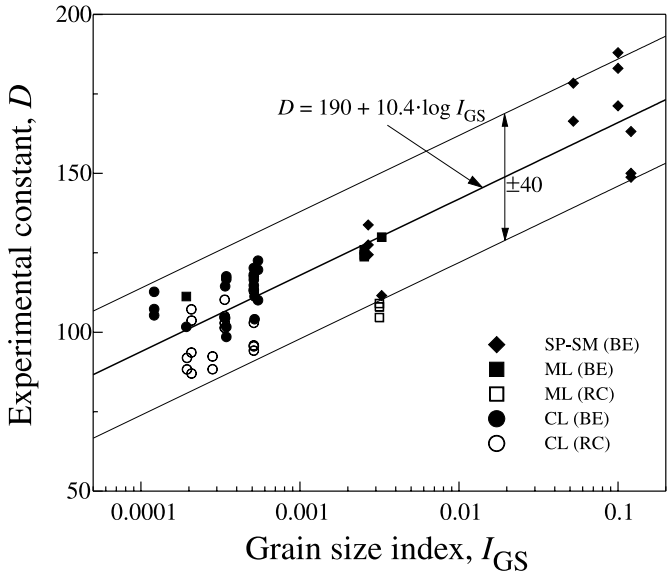

(1) A well-defined distinction in the mechanical response between sands and silts was difficult to assess, whereas the distinction between SM-SP-ML and CL was clearly evident.

(2) The 1D and very small strain stiffness, both dependent on the current void ratio and the effective stress level, could be clearly related to the grading properties through I_{GS}.

(3) Critical state parameters, such as the slopes of the CSL in the e – log p' and q–p' planes, and the reference void ratio (or specific volume), showed a well-defined dependence on the grain-size composition expressed by I_{GS}.

(4) The maximum dilatancy at failure or, alternatively, the peak friction angle, both dependent on the void ratio and the mean effective stress level at failure, can be expressed as a function of the state parameter, which also appeared to be dependent on grain-size composition. This latter aspect

requires further experimental research to be fully validated however.

Finally, based on all of the above considerations, it could be observed that the use of the grain-size index may represent a valid additional parameter for use in the mechanical characterization of natural highly heterogeneous and interbedded soils, formed by sediments coming from a common mineralogical origin, such as those of the Venice lagoon.

References

Andersen, A., and Kolstad, P. 1979. The NGI 54 mm samplers for undisturbed sampling of clays and representative sampling of coarser materials. *In* Proceedings of the International Symposium on Soil Sampling, Singapore, pp. 13–21.

Becker, D.E., Crooks, J.H.A., Been, K., and Jefferies, M.G. 1987. Work as a criterion for determining *in situ* and yield stresses in clays. Canadian Geotechnical Journal, **24**: 549–564.

Been, K., and Jefferies, M.G. 1985. A state parameter for sands. Géotechnique, **35**(2): 91–112.

Been, K., Jefferies, M.G., and Hachey, J. 1991. The critical state of sands. Géotechnique, **41**(3): 365–381.

Biarez, J., and Hicher, P.I. 1994. Elementary soils mechanics: saturated remoulded soils. A.A. Balkema, Rotterdam.

Bolton, M.D. 1986. The strength and dilatancy of sands. Géotechnique, **36**(1): 65–78.

Bolton, M.D. 1987. Discussion, The strength and dilatancy of sands. Géotechnique, **37**(2): 225–226.

Cola, S., and Simonini, P. 1999. Some remarks on the behavior of Venetian silts, *In* Proceedings of the 2nd International Symposium on Pre-failure Behaviour of Geomaterials, IS Torino 99, A.A. Balkema, Rotterdam, pp. 167–174.

Hardin, B.O., and Black, W.L. 1969. Vibration modulus of normally consolidated clay. Journal of Soil Mechanics and Foundations Division, ASCE, **95**(SM1): 33–65.

Hardin, B.O., and Drnevich, V.P. 1972. Shear modulus and damping in soils: design equations and curves. Journal of Soil Mechanics and Foundations Division, ASCE, **98**(SM7): 667–692.

Holtz, R.D., Jamiolkowski, M., and Lancellotta, R. 1986. Lessons from oedometer tests on high quality samples. Journal of Geotechnical Engineering, ASCE, **112**(8): 768–776.

Houlsby, G.T. 1991. How the dilatancy of soils affects their behaviour. *In* Proceedings of the 10th European Conference on Soil Mechanics and Foundation Engineering (ECSMFE), Florence, A.A. Balkema, Rotterdam. Vol. 4, pp. 1189–1202.

Ishihara, K., Tatsuoka, F., and Yashuda, S. 1975. Undrained strength and deformation of sand under cyclic stresses. Soils and Foundations, **15**(1): 29–44.

Jamiolkowski, M., Lancellotta, R., and Lo Presti, D.C.F. 1994. Remarks on the stiffness at small strains of six Italian clays. *In* Proceedings of the Symposium on the Prefailure Deformation Characteristics of Geomaterials, A.A. Balkema, Rotterdam. Vol. 2, pp. 817–836.

Janbu, N. 1963. Soil compressibility as determined by oedometer and triaxial tests. *In* Proceedings of the 3rd European Conference on Soil Mechanics and Foundation Engineering (ECSMFE), Wiesbaden, Richard Bacht Grafische-Betriebe Und Verlag Gmbh, Essen. Vol. 1, pp. 245–251.

Jefferies, M.J. 1993. Nor-sand: a simple critical state model for sand. Géotechnique, **43**(1): 91–103.

Jefferies, M., and Been, K. 2000. Implication for critical state theory from isotropic compression of sand. Géotechnique, **50**(4): 419–429.

Lee, K.L., and Seed, H.B. 1967. Drained strength characteristics of sands. Journal of Soil Mechanics and Foundations Division, ASCE, **99**(SM6): 117–141.

Marchetti, S. 1980. In situ tests by flat dilatometer. Journal of Geotechnical Engineering, ASCE, **106**(GT3): 299–321.

Mc Dowell, G.R. 1996. Classic soil mechanics, Ph.D. dissertation, Cambridge University.

Mc Dowell, G.R., and Bolton, M.D. 1998. On the micromechanics of crushable aggregates. Géotechnique, **8**(5): 667–679.

Miura, K., Kenichi, M., Furukawa, M., and Shosuke, T. 1997. Physical characteristics of sand with different primary properties. Soils and Foundations, **37**(3): 53–63.

Pestana, J.M., and Whittle, A.J. 1996. Compression model for cohesionless soils. Géotechnique, **45**(4): 611–632.

Ricceri, G. 1997. Geotechnical problems for the barriers. *In* Proceedings of the Symposium on "Venice and Florence: a complex dialogue with water," 24 May, Florence, International Technical Committee on Large Dams (ITCOLD), Italian Committee for Large Dams, Patron, Bologna, pp. 55–72.

Ricceri, G., and Butterfield, R. 1974. An analysis of compressibility data from a deep borehole in Venice, Géotechnique, **24**(2): 175–192.

Ricceri, G., Simonini, P., and Cola, S. 2002. Applicability of piezocone and dilatometer to characterize the soils of the Venice lagoon. Geotechnical and Geological Engineering, **20**: 89–121.

Rowe, P.W. 1962. The stress-dilatancy relation for static equilibrium of an assembly of particles in contact. Proceedings of the Royal Society, Vol. 269, Series A, pp. 500–527.

Rowe, P.W. 1973. Soil mechanic aspect of the cores of the deep borehole VE1 in Venice. A critical analysis and recommended future investigations. Technical Report No. 57. National Research Council, Venice.

Shibuya, S., and Tanaka, H. 1996. Estimate of elastic shear modulus in Holocene soil deposits. Soils and Foundations, **36**(4): 45–55.

Simonini, P., and Cola, S. 2000. Use of piezocone to predict maximum stiffness of Venetian soils. Journal of Geotechnical and Geoenvironmental Engineering, ASCE, **126**(4): 378–382.

Smith, M.J., and Houlsby, G.T. 1995. Interpretation of Marchetti dilatometer in clay. *In* Proceedings of the 11th European Conference on Soil Mechanics and Foundation Engineering (ECSMFE), Copenhagen, Danish Geotechnical Society, Vol. 1, DGF-Bulletin 11, pp. 247–252.

Tatsuoka, F., and Ishihara, K. 1974. Drained deformation of sand under cyclic stress reversing direction. Soils and Foundations, **14**(3): 51–65.

Tatsuoka, F., and Shibuya, S. 1992. Deformation characteristics of soil and rocks from field and laboratory tests. Report of the Institute of Industrial Science, Serial No. 235, University of Tokyo.

Wood, D., Belkeir, K., and Liu, D.F. 1994. Strain softening and state parameter for sand modelling. Géotechnique, **44**(2): 335–339.

Wroth, C.P., and Bassett, R.H. 1965. A stress–strain relationship for the shearing behaviour of sand. Géotechnique, **15**(1): 32–56.